

Chapter 2

Modelling of Fluid Flow and Heat Transfer in Rotating-Disk Systems

2.1 Differential and Integral Equations

2.1.1 Differential Navier–Stokes and Energy Equations

We will consider here stationary axisymmetric fluid flow over disks rotating with a sufficiently high angular velocity so that effects of gravitational forces on momentum transfer are rather low. In a stationary cylindrical coordinate system arranged in such a way that a disk or a system of disks rotate around its axis of symmetry coinciding with the axis z , while the point $z=0$ is located on a surface of the disk (Fig. 2.1), laminar fluid flow and heat transfer are described by Eqs. (1.31), (1.32), (1.33), (1.34) and (1.35) simplified accounting for the conditions $F_r = F_\varphi = F_z = 0$ [41, 138, 139]:

$$v_r \frac{\partial v_r}{\partial r} + v_z \frac{\partial v_r}{\partial z} - \frac{v_\varphi^2}{r} = -\frac{1}{\rho} \frac{\partial p}{\partial r} + \nu \left(\frac{\partial^2 v_r}{\partial r^2} + \frac{1}{r} \frac{\partial v_r}{\partial r} - \frac{v_r}{r^2} + \frac{\partial^2 v_r}{\partial z^2} \right), \quad (2.1)$$

$$v_r \frac{\partial v_\varphi}{\partial r} + v_z \frac{\partial v_\varphi}{\partial z} + \frac{v_r v_\varphi}{r} = \nu \left(\frac{\partial^2 v_\varphi}{\partial r^2} + \frac{1}{r} \frac{\partial v_\varphi}{\partial r} - \frac{v_\varphi}{r^2} + \frac{\partial^2 v_\varphi}{\partial z^2} \right), \quad (2.2)$$

$$v_r \frac{\partial v_z}{\partial r} + v_z \frac{\partial v_z}{\partial z} = -\frac{1}{\rho} \frac{\partial p}{\partial z} + \nu \left(\frac{\partial^2 v_z}{\partial r^2} + \frac{1}{r} \frac{\partial v_z}{\partial r} + \frac{\partial^2 v_z}{\partial z^2} \right), \quad (2.3)$$

$$\frac{\partial v_r}{\partial r} + \frac{v_r}{r} + \frac{\partial v_z}{\partial z} = 0, \quad (2.4)$$

$$\frac{\partial T}{\partial t} + v_r \frac{\partial T}{\partial r} + v_z \frac{\partial T}{\partial z} = a \frac{1}{r} \frac{\partial}{\partial r} \left(r \frac{\partial T}{\partial r} \right) + a \frac{\partial^2 T}{\partial z^2}. \quad (2.5)$$

For turbulent flow with account for the conditions $F_r = F_\varphi = F_z = 0$, Eqs. (1.36), (1.37), (1.38) and (1.39) take the following form [41, 138, 139]:

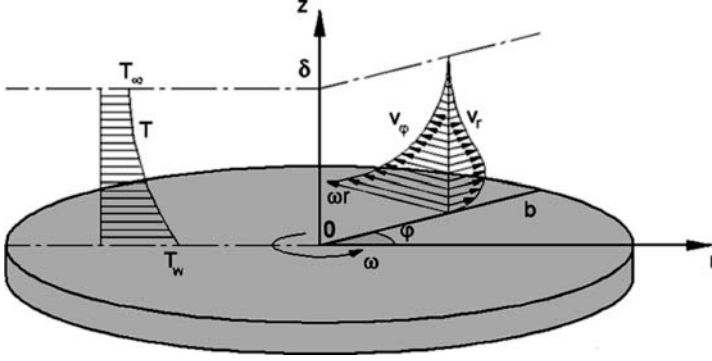


Fig. 2.1 Geometrical arrangement and main parameters of the problem of fluid flow and heat transfer over a rotating disk in still air.

$$v_r \frac{\partial v_r}{\partial r} + v_z \frac{\partial v_r}{\partial z} - \frac{v_\varphi^2}{r} = -\frac{1}{\rho} \frac{\partial p}{\partial r} + \nu \left(\nabla^2 v_r - \frac{v_r}{r^2} \right) + \frac{1}{r} \frac{\partial}{\partial r} \left(-\overline{v_r'^2} \right) + \frac{\partial}{\partial z} \left(-\overline{v_r' v_z'} \right) - \frac{1}{r} \left(-\overline{v_r'^2} \right), \quad (2.6)$$

$$v_r \frac{\partial v_\varphi}{\partial r} + v_z \frac{\partial v_\varphi}{\partial z} + \frac{v_r v_\varphi}{r} = \nu \left(\nabla^2 v_\varphi - \frac{v_\varphi}{r^2} \right) + \frac{\partial}{\partial r} \left(-\overline{v_r' v_\varphi'} \right) + \frac{\partial}{\partial z} \left(-\overline{v_\varphi' v_z'} \right) + \frac{2}{r} \left(-\overline{v_r' v_\varphi'} \right), \quad (2.7)$$

$$v_r \frac{\partial v_z}{\partial r} + v_z \frac{\partial v_z}{\partial z} = -\frac{1}{\rho} \frac{\partial p}{\partial z} + \nu \left(\nabla^2 v_z \right) + \frac{1}{r} \frac{\partial}{\partial r} \left(-\overline{v_r' v_z'} \right) + \frac{\partial}{\partial z} \left(-\overline{v_z'^2} \right), \quad (2.8)$$

$$\frac{\partial T}{\partial t} + v_r \frac{\partial T}{\partial r} + v_z \frac{\partial T}{\partial z} = \frac{1}{r} \frac{\partial}{\partial r} \left[r \left(a \frac{\partial T}{\partial r} - \overline{v_r' T'} \right) \right] + \frac{\partial}{\partial z} \left(a \frac{\partial T}{\partial z} - \overline{v_z' T'} \right). \quad (2.9)$$

In a rotating coordinate system connected with a disk, Eqs. (2.1), (2.2) and (2.3) for laminar flow can be transformed as follows [138, 139]:

$$v_r \frac{\partial v_r}{\partial r} + v_z \frac{\partial v_r}{\partial z} - \frac{v_\varphi^2}{r} - 2\omega v_\varphi - \omega^2 r = -\frac{1}{\rho} \frac{\partial p}{\partial r} + \nu \left(\frac{\partial^2 v_r}{\partial r^2} + \frac{1}{r} \frac{\partial v_r}{\partial r} - \frac{v_r}{r^2} + \frac{\partial^2 v_r}{\partial z^2} \right), \quad (2.10)$$

$$v_r \frac{\partial v_\varphi}{\partial r} + v_z \frac{\partial v_\varphi}{\partial z} + \frac{v_r v_\varphi}{r} + 2\omega v_r = \nu \left(\frac{\partial^2 v_\varphi}{\partial r^2} + \frac{1}{r} \frac{\partial v_\varphi}{\partial r} - \frac{v_\varphi}{r^2} + \frac{\partial^2 v_\varphi}{\partial z^2} \right), \quad (2.11)$$

$$v_r \frac{\partial v_z}{\partial r} + v_z \frac{\partial v_z}{\partial z} = -\frac{1}{\rho} \frac{\partial p}{\partial z} + \nu \left(\frac{\partial^2 v_z}{\partial r^2} + \frac{1}{r} \frac{\partial v_z}{\partial r} + \frac{\partial^2 v_z}{\partial z^2} \right). \quad (2.12)$$

The terms $2\omega v_\varphi$ and $2\omega v_r$ are the projections of the Coriolis forces onto the axes r and φ , respectively, while the term $\omega^2 r$ is the projection of centrifugal force onto the axis r (all divided by ρ). For turbulent flow, Eqs. (2.6), (2.7) and (2.8) can be rewritten in the same way [138, 139].

2.1.2 Differential Boundary Layer Equations

In the boundary layer approximation, it is assumed that [41, 138, 139]

- (a) the velocity component v_z is by order of magnitude lower than the components v_r and v_φ ;
- (b) the rate of variation of the velocity, pressure and temperature in the direction of the axis z is much larger than the rate of their variation in the direction of the axis r ;
- (c) static pressure is constant in the z -direction.

The continuity equation (2.4) remains invariable, while the other equations of the system (2.6), (2.7), (2.8) and (2.9) take the following form [41, 138, 139]:

$$v_r \frac{\partial v_r}{\partial r} + v_z \frac{\partial v_r}{\partial z} - \frac{v_\varphi^2}{r} = -\frac{1}{\rho} \frac{\partial p}{\partial r} + \frac{1}{\rho} \frac{\partial \tau_r}{\partial z}, \quad (2.13)$$

$$v_r \frac{\partial v_\varphi}{\partial r} + v_z \frac{\partial v_\varphi}{\partial z} + \frac{v_r v_\varphi}{r} = \frac{1}{\rho} \frac{\partial \tau_\varphi}{\partial z}, \quad (2.14)$$

$$\frac{1}{\rho} \frac{\partial p}{\partial z} = 0, \quad (2.15)$$

$$\frac{\partial T}{\partial t} + v_r \frac{\partial T}{\partial r} + v_z \frac{\partial T}{\partial z} = -\frac{1}{\rho c_p} \frac{\partial q}{\partial z}, \quad (2.16)$$

$$\tau_r = \mu \frac{\partial v_r}{\partial z} - \rho \overline{v'_r v'_\varphi}, \quad (2.17)$$

$$\tau_\varphi = \mu \frac{\partial v_\varphi}{\partial z} - \rho \overline{v'_\varphi v'_z}, \quad (2.18)$$

$$q = -(\lambda \frac{\partial T}{\partial z} - \rho c_p \overline{T' v'_z}). \quad (2.19)$$

In Eqs. (2.17), (2.18) and (2.19), only those components of the turbulent shear stresses and heat fluxes are taken into account, whose input into momentum and heat transfer is the most important. It is natural that the pressure in the boundary layer is assumed to be equal to its value outside of the boundary layer in the region of potential flow $p=p_\infty$.

The equation of the stationary thermal boundary layer looks as follows:

$$v_r \frac{\partial T}{\partial r} + v_z \frac{\partial T}{\partial z} = -\frac{1}{\rho c_p} \frac{\partial q}{\partial z}. \quad (2.20)$$

The system of Eqs. (2.13), (2.14), (2.15), (2.16), (2.17), (2.18) and (2.19) is completed by an equation in the region of potential flow outside of the boundary layer, where velocity components and pressure p_∞ are considered invariable in the z -direction:

$$\frac{1}{2} \frac{dv_{r,\infty}^2}{dr} - \frac{v_{\varphi,\infty}^2}{r} = -\frac{1}{\rho} \frac{dp_\infty}{dr}. \quad (2.21)$$

2.1.3 Integral Boundary Layer Equations

These equations (which are in fact integral–differential equations) for stationary fluid flow and heat transfer can be derived from Eqs. (2.13), (2.14), (2.15), (2.17), (2.18), (2.19) and (2.20) with allowance for Eqs. (2.4) and (2.21) in the following form [41, 138, 139]:

$$\begin{aligned} \frac{d}{dr} \left[r \int_0^\delta v_r (v_{r,\infty} - v_r) dz \right] + r \frac{dv_{r,\infty}}{dr} \int_0^\delta (v_{r,\infty} - v_r) dz \\ - \int_0^\delta (v_{\varphi,\infty}^2 - v_\varphi^2) dz = r\tau_{wr}/\rho, \end{aligned} \quad (2.22)$$

$$\frac{d}{dr} \left[r^2 \int_0^\delta v_r (v_\varphi - v_{\varphi,\infty}) dz \right] + \frac{\dot{m}_d}{2\pi\rho} \frac{d}{dr} (rv_{\varphi,\infty}) = -r^2\tau_{w\varphi}/\rho, \quad (2.23)$$

or

$$\frac{d}{dr} \left[r^2 \int_0^\delta v_r v_\varphi dz \right] + rv_{\varphi,\infty} \frac{d}{dr} \left(\frac{\dot{m}_d}{2\pi\rho} \right) = -r^2\tau_{w\varphi}/\rho, \quad (2.24)$$

$$\frac{d}{dr} \left[r \int_0^{\delta_T} v_r (T - T_\infty) dz \right] + \frac{dT_\infty}{dr} \cdot \frac{\dot{m}_{d,T}}{2\pi\rho} = rq_w/(\rho c_p). \quad (2.25)$$

Equations (2.22), (2.23) and (2.25) can be rewritten as follows [41, 138, 139, 180]:

$$\frac{d}{dr} \left(v_{r,\infty}^2 r \delta \bar{\delta}_r^{**} \right) + v_{r,\infty} r \delta \frac{dv_{r,\infty}}{dr} \bar{\delta}_r^* - v_{\varphi,\infty}^2 \delta \bar{\delta}_\varphi^{**} = r\tau_{wr}/\rho, \quad (2.26)$$

$$\frac{d}{dr} [\delta r^2 (\omega r)^2 \bar{\delta}_{\varphi r}^{**}] + \frac{\dot{m}_d}{2\pi\rho} \frac{d}{dr} (rv_{\varphi,\infty}) = -r^2\tau_{w\varphi}/\rho, \quad (2.27)$$

$$\frac{d}{dr} [\omega r^2 \delta \bar{\delta}_T^{**} (T_w - T_\infty)] + \frac{dT_\infty}{dr} \cdot \frac{\dot{m}_{d,T}}{2\pi\rho} = rq_w/(\rho c_p), \quad (2.28)$$

where

$$\bar{\delta}_r^* = \int_0^1 (1 - \tilde{v}_r) d\xi, \quad \bar{\delta}_r^{**} = \int_0^1 \tilde{v}_r (1 - \tilde{v}_r) d\xi, \quad \bar{\delta}_\varphi^{**} = \int_0^1 \left(1 - \frac{v_\varphi^2}{v_{\varphi,\infty}^2} \right) d\xi, \quad (2.29)$$

$$\bar{\delta}_{\varphi r}^{**} = \int_0^1 \frac{v_r(v_\varphi - v_{\varphi,\infty})}{(\omega r)^2} d\xi, \quad \tilde{v}_r = v_r/v_{r,\infty}. \quad (2.30)$$

2.2 Differential Methods of Solution

2.2.1 Self-Similar Solution

For laminar flows over a single rotating disk, exact solutions of the Navier–Stokes and energy equations were obtained in works [33, 41, 55, 58, 80, 106, 138, 139, 158, 199] using the following self-similar variables:

$$\begin{aligned} v_r &= (a + \omega)rF(\zeta), \quad v_z = \sqrt{(a + \omega)\nu}H(\zeta), \quad v_\varphi = (a + \omega)rG(\zeta), \\ p &= -\rho\nu\omega P(\zeta), \quad \theta = (T - T_\infty)/(T_w - T_\infty), \quad \zeta = z\sqrt{(a + \omega)/\nu}, \end{aligned} \quad (2.31)$$

under the boundary conditions

$$\zeta \rightarrow \infty: \quad v_{r,\infty} = ar, \quad v_{z,\infty} = -2az, \quad v_{\varphi,\infty} = \Omega r, \quad \beta = \Omega/\omega = \text{const}, \quad \theta = 0, \quad (2.32)$$

$$\zeta = 0: \quad F = H = 0, \quad G = 1, \quad \theta = 1, \quad (2.33)$$

$$\zeta = 0: \quad T_w = T_{ref} + c_{0w}r^{n_*}, \quad T_\infty = T_{ref} + c_{0\infty}r^{n_*} \text{ or } T_\infty = T_{ref} + \beta c_{0w}r^{n_*}, \quad (2.34)$$

where c_0 , c_{0w} , $c_{0\infty}$ and n_* are constants. Boundary conditions (2.34) can be transformed as follows:

$$\Delta T = T_w - T_\infty = c_0 r^{n_*} \quad (\text{for } c_0 = c_{0w} - c_{0\infty}), \quad (2.35)$$

or

$$\Delta T = c_{0w}(1 - \beta)r^{n*}. \quad (2.36)$$

Taking into account Eq. (2.21) for the radial pressure gradient in the region of potential flow, Eqs. (2.1), (2.2), (2.3) and (2.4) and (2.20) take the following self-similar form:

$$F^2 - G^2 + F'H = \frac{N^2 - \beta^2}{(1 + N)^2} + F'', \quad (2.37)$$

$$2FG + G'H = G'', \quad (2.38)$$

$$HH' = P' + H'', \quad (2.39)$$

$$2F + H' = 0, \quad (2.40)$$

$$\theta'' - \text{Pr} (n_* F\theta + H\theta') = 0, \quad (2.41)$$

where $N=a/\omega=const$ (and, naturally, turbulence components were neglected). It is impossible to assign simultaneously non-zero values of β and N in Eq. (2.37), because in this case the derivative of the component $F(\zeta)$ does not tend to zero on the outer boundary of the boundary layer. However, Eq. (2.37) still holds either for $N \neq 0$ and $\beta=0$ or for $\beta \neq 0$ and $N=0$.

In the past, solutions of the Eqs. (2.37), (2.38), (2.39), (2.40) and (2.41) have been obtained with the help of individually developed computer codes based on expansions in power or exponential series [80], use of the shooting method [58, 106, 138, 199], etc. Currently, standard computer mathematics software like MathCAD, etc. allows programming solutions of the systems of equations like Eqs. (2.37), (2.38), (2.39), (2.40) and (2.41) with the help of the user interface options.

As shown in works [41, 138, 139], a self-similar form of the energy equation with account for dissipation effects imposes restriction onto the boundary conditions (2.34), (2.35) and (2.36): in this case, one can use only the value of the exponent $n_*=2$. Since effects of radial heat conduction and energy dissipation in air cooling systems at sub-sonic speeds are negligible, the advantage to use arbitrary n_* values in the thermal boundary layer equation (2.41) by far compensates very minor losses involved because of neglecting the aforementioned terms in the energy equation.

Exact solutions of Eqs. (2.37), (2.38), (2.39), (2.40) and (2.41) provide a reliable database useful, among other applications, in validations of CFD codes and models aimed at solving much more complicated physical problems. Use of the self-similar solutions also enables obtaining approximate analytical solutions for problems with boundary conditions different from Eqs. (2.32), (2.33), (2.34), (2.35) and (2.36).

2.2.2 Approximate Analytical Methods for Laminar Flow Based on Approximations of Velocity Profiles

The method of Slezkin-Targ was used in the work [41] to model laminar fluid flow over a free rotating disk at $\beta=0$ and $N=0$, as well as for the case of $N=const$ and $\beta=0$. Velocity profiles derived for the case of $\beta=0$ and $N=0$ were described by the sixth-order power polynomials, which in view of the necessity to further develop the method would inevitably result in obtaining inconvenient and cumbersome relations for the Nusselt number. Decreasing the order of the approximating polynomial to the third order resulted, in the case of $N=const$ and $\beta=0$, in noticeable errors in calculations of surface friction, which were equal to approximately 25% at $N=5$ and increased sharply with the further increasing values of N .

The author of the work [4] obtained an approximate solution for the velocity components in laminar fluid flow over a free rotating disk in a form of a rather complex combination of exponential and logarithmic functions. The method was not extended to include the heat transfer problem as well as to take into consideration the boundary condition (2.32). It should be expected that the development of the method [4] in this direction would result in obtaining even more inconvenient and cumbersome relations, in particular, for the Nusselt number, than those resulting from the approach of Slezkin-Targ [41].

The approximate solution [83] for porous injection through a rotating disk has a form of a combined expansion in power and exponential series. The authors did not generalize their method for more complex cases; however, it is obvious that their approach has the same deficiencies as the methods of [4, 41].

It can be thus concluded that velocity, pressure and temperature profiles in laminar boundary layers over a rotating disk are so much complicated from the mathematical point of view that a search of their rather accurate analytical approximation is inexpedient. As shown below, a combination of an integral method with the data of self-similar solutions can result in obtaining rather simple and accurate approximate analytical solutions for surface friction coefficients and Nusselt numbers.

2.2.3 Numerical Methods

Authors of [136] solved boundary layer equations (2.13), (2.14), (2.15), (2.16), (2.17), (2.18), (2.19) and (2.20) with the help of a finite-difference method employing a modified algebraic model of turbulent viscosity by Cebeci-Smith [22]. For the case of laminar steady-state heat transfer with tangential non-uniformity of heating of the disk surface, Eq. (1.30) was reduced to a two-dimensional equation in works [205, 206] using modified variables (2.31). A steady-state axisymmetric problem with a localized heat source was modelled in the work [137] with the help of Eq. (2.9). In both aforementioned cases, a finite-difference technique was used. Equations (2.6), (2.7), (2.8) and (2.9) were used to model both laminar and turbulent flow and heat transfer in cavities between parallel rotating disks [78, 79, 145, 148,

151]. Authors of [148] applied a finite-difference method for a two-dimensional laminar steady-state problem. In works [25, 78, 79, 90, 145, 225], an in-house computer code based on the finite-volume method was used to solve Eqs. (2.6), (2.7), (2.8) and (2.9) closed with low Reynolds number k - ε models of turbulence [101, 128, 129]. Large eddy simulation (LES) approach was used in the work [224] to model a three-dimensional stationary turbulent flow over a rotating disk, and turbulent flow and heat transfer over a single disk in air flow parallel to the disk surface (non-symmetrical flow) in works [220, 221]. Author of [38] used a finite-difference method to solve the Navier–Stokes equations closed with a k - ε turbulence model by [100] as applied to three-dimensional flow of a carrying phase (air) in a rotating-disk grinder of solid particles.

Authors of [151, 152] used a commercial CFD code Fluent to solve Eqs. (2.6), (2.7), (2.8) and (2.9) closed with an RNG k - ε turbulence model. Commercial CFD code Phoenix was used by the authors of [188] to simulate stationary turbulent one-phase flow in a rotating-disk air cleaner using a standard k - ε turbulence model. In the work [61], modelling of laminar conjugate transient heat transfer of a free rotating disk was performed using a commercial CFD code CFX.

Numerical methods are the most universal tool of mathematical modelling inevitably used in simulations of problems with complex geometry, arbitrary boundary conditions, etc. Relative complications in use of such methods are significant time consumption for one run (often tens of hours), generation of a computational mesh (often weeks), sometimes lack of convergence of the numerical solution, etc. Therefore, use of such methods is not justified for relatively simple problems that can be solved by means of simpler approaches.

A general disadvantage of the differential methods (which one can nevertheless comply with) is obtaining solution in a numerical form that is usually a certain inconvenience in comparison with analytical solutions.

2.3 Integral Methods of Solution

2.3.1 Momentum Boundary Layer

The essence of integral methods consists in solving Eqs. (2.22), (2.23), (2.24), (2.25), (2.26), (2.27) and (2.28) closed with models for the velocity profiles and shear stress components on the wall for the momentum boundary layer, as well as for the temperature profiles (or enthalpy thickness) and wall heat flux for the thermal boundary layer.

The most perfect integral method among those known in the literature is the method of [138, 139], which developed ideas of the authors of [41, 80]. A key point of the method [138, 139] consists in use of a generalized form of the models that takes into account existence of laminar or turbulent flow via assigning particular numerical values to certain parameters of the model. This is a confirmation of the idea expressed by Loytsyanskiy still in the year of 1945 [113], who said that there

exists “an analogy between basic characteristics of laminar and turbulent boundary layers”.

In the boundary layer, the radial v_r and tangential v_φ velocity components correlate with each other. This correlation is described by the formula [163]

$$\bar{v}_r = \bar{v}_\varphi \tan\varphi. \quad (2.42)$$

For flows, where radial velocity of the flow outside of the boundary layer can be neglected, i.e. for $v_{r,\infty}=0$, authors of [138, 139] specified the velocity profiles as

$$\bar{v}_\varphi = 1 - g(\xi), \quad \bar{v}_r = \alpha f(\xi), \quad (2.43)$$

where functions $g(\xi)$ and $f(\xi)$ expressed in terms of the independent variable $\xi=z/\delta$ were assumed to be self-similar (independent of the coordinate r).

For a laminar boundary layer, functions $g(\xi)$ and $f(\xi)$ can be expressed as

$$g(\xi) = G_0(\xi), \quad f(\xi) = F_0(\xi)/\alpha_0, \quad (2.44)$$

where functions $G_0(\xi)$ and $F_0(\xi)$ are tabulated [41, 138, 139] being a solution of the problem of fluid flow over a free rotating disk in the self-similar form of Eqs. (2.37), (2.38), (2.39) and (2.40) at $N=0$ and $\beta=0$.

For a turbulent boundary layer, the following power-law approximations were used in the works [41, 138, 139]:

$$g(\xi) = 1 - \xi^n, \quad (2.45)$$

$$f(\xi) = \xi^n(1 - \xi), \quad \tan\varphi = \alpha(1 - \xi), \quad (2.46)$$

where $n=1/5-1/10$. The models (2.45) and (2.46) were formulated by von Karman [80] in 1921 for the first time by analogy with the model for turbulent flow in a round pipe and over a flat plate [158]. The exponent n is assumed to be known and selected depending on the characteristic Reynolds number (Figs. 2.2, 2.3 and 2.4).

Model (2.45) for the turbulent boundary layer was also used by the authors of [7, 122, 130]. A more accurate approximation of the function $f(\xi)$ in turbulent flow is the expression used by the authors of [32, 70, 118, 196]:

$$f(\xi) = \xi^n(1 - \xi)^2, \quad \tan\varphi = \alpha(1 - \xi)^2, \quad (2.47)$$

which, however, has not been used so widely because of somewhat increased complexity in integrating the terms in the left-hand side of Eqs. (2.22), (2.23) and (2.24).

For flows at $N=const$, the following relation was used in [212]:

$$\tan\varphi = \alpha + (N - \alpha) \xi. \quad (2.48)$$

Authors of [41, 69] used the following expressions:

Fig. 2.2 Profiles of the non-dimensional tangential velocity in the turbulent boundary layer over a free rotating disk. Calculation by Eq. (2.45) [163], $1 - n = 1/7$, $2 - 1/8$, $3 - 1/9$. Experiments: $4 - Re_\omega = (0.4 - 1.6) \cdot 10^6$ [111], $5 - (0.6 - 1.0) \cdot 10^6$ [63], $6 - (0.65 - 1.0) \cdot 10^6$ [46]. Here $\delta_\varphi^{**} = \int_0^b \frac{v_\varphi}{\omega r} (1 - \frac{v_\varphi}{\omega r}) dz$ (definition of [26, 46, 47, 63, 111]).

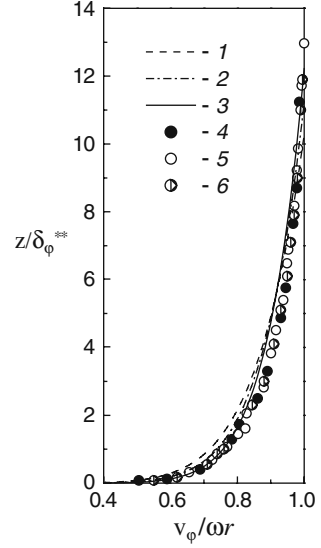
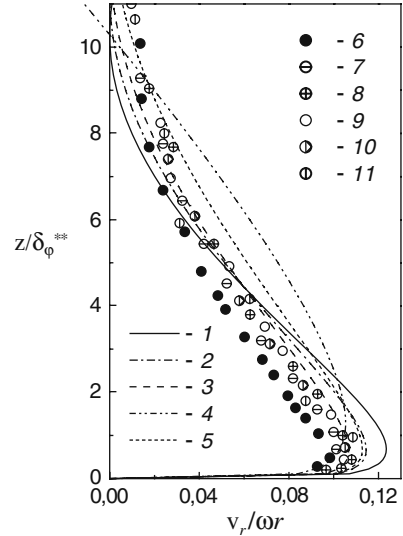


Fig. 2.3 Profiles of the non-dimensional radial velocity in the turbulent boundary layer over a free rotating disk. Calculation by Eq. (2.47) (or Eq. (2.63)) [163], $1 - n = 1/7$, $2 - 1/8$, $3 - 1/9$, $4 - 1/7$, von Karman's Eq. (2.46) [80], $5 - 1/7$, Eq. (2.50) for $b=0.7$, $c=1.2$, $\alpha=0.2003$. Experiments: $6 - Re_\omega = 0.4 \cdot 10^6$, $7 - 0.65 \cdot 10^6$, $8 - 0.94 \cdot 10^6$, $9 - 1.6 \cdot 10^6$ [111], $10 - 0.6 \cdot 10^6$, $11 - 1.0 \cdot 10^6$ [63]



$$f(\xi) = \xi^n (1 - \xi^{n/m}), \quad \tan \varphi = \alpha (1 - \xi^{n/m}), \quad (2.49)$$

where constants n and m could be varied independently. However, model (2.49) has not been further developed because of its excessive complexity.

Authors of [1, 2] used a trigonometric function to approximate the tangent of the flow swirl angle

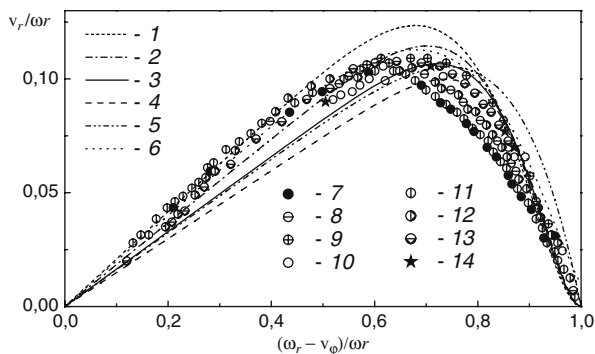


Fig. 2.4 Correlation between the radial and tangential components in the boundary layer. Calculation by Eq. (2.64) at $L=2$ (curves 1–4) or $L=1$ (curve 5) [163]: 1 – $n=1/7$, 2 – $1/8$, 3 – $1/9$, 4 – $1/10$, 5 – $1/7$, von Karman's method [80], 6 – $1/7$, Eq. (2.50) for $b=0.7$, $c=1.2$, $\alpha=0.2003$. Experiments: 7 – $Re_\omega=0.4 \cdot 10^6$, 8 – $0.65 \cdot 10^6$, 9 – $0.94 \cdot 10^6$, 10 – $1.6 \cdot 10^6$ [111], 11 – $0.4 \cdot 10^6$, 12 – $0.6 \cdot 10^6$, 13 – $1.0 \cdot 10^6$ [63], 14 – $2.0 \cdot 10^6$ [21].

$$\tan \varphi = \alpha [(1 - \sin^b(c\xi))], \quad (2.50)$$

where constants b and c take the values $b=0.7$, $c=0.12$ at $n=1/7$, and $b=0.697$, $c=0.117$ at $n=1/8$. Authors [1, 2] asserted that the model (2.50) allows to attain better agreement with experiments for a free rotating disk than with von Karman's approach (2.45), (2.46).

Analysis shows, however, that the values of the constants b and c given in [1] are erroneous. For example, keeping the value $b=0.7$ at $n=1/7$ invariable, it is necessary to use the value of $c=1.2$ (Figs. 2.3 and 2.4). However, the model [1, 2] has not been further developed to include heat transfer, apparently, because resulting expressions for the Nusselt number obtained on the base of Eq. (2.50) would have been too cumbersome.

In works [73–75], it was assumed for $N=\text{const}$ that

$$\tan \varphi = \alpha (1 - \xi) + \kappa, \quad (2.51)$$

where $\kappa = \dot{m} / [2\pi\rho sr(1 - \beta)\omega r]$. This approximation is worse than Eq. (2.48), because it does not agree with the apparent condition $\tan \varphi_w = \alpha$ and complicates the solution of Eqs. (2.22) and (2.23).

The author of [72] used a relation $\tan \varphi = cN$, where $N = \dot{m} / (2\pi\rho sr)$, with the constant c varying from the value 1.0 at the inlet to a cavity between parallel co-rotating disks to 1.22 in the region of stabilized flow. This relation was used for large values of $v_{r,\infty}$ and $v_{\phi,\infty} \approx 0$. The disadvantages of this approach are lack of agreement with the boundary condition $\tan \varphi_w = \alpha$ and involvement of a new empirical constant c .

Thus, models (2.49), (2.50) and (2.51) have shown worse performance than Eqs. (2.42), (2.43), (2.44), (2.45), (2.46), (2.47) and (2.48).

After integration of the terms in the left-hand side of Eqs. (2.22) and (2.23) with account for Eqs. (2.42), (2.43), (2.44), (2.45), (2.46), (2.47) and (2.48), the unknowns to be found are parameters $\alpha(r)$ and $\delta(r)$ for a prescribed distribution of $\beta(r)$ or $\alpha(r)$ and $\beta(r)$ for a prescribed $\delta(r)$. Under conditions $N=const$ or $\beta=const$, the value of α is also constant, while the value of δ is either also constant in laminar flow or has a form of a power-law function of r in turbulent flow [41, 138, 139].

Apart from the works [138, 139], no other author has developed an integral method for laminar flow for an arbitrary distribution of $\beta(r)$.

In frames of the approach with power-law approximation of the velocity profiles, shear stresses τ_{wr} and $\tau_{w\varphi}$ in the right-hand side of Eqs. (2.22), (2.23) and (2.24) are determined by the following equations [41, 138, 139]:

$$\tau_{wr} = -\alpha\tau_{w\varphi}, \quad \tau_{w\varphi} = -\text{sgn}(1 - \beta)\tau_w(1 + \alpha^2)^{1/2}, \quad (2.52)$$

$$c_f = C_n^{-2/(n+1)} \cdot Re_{V_*}^{-2n/(n+1)}, \quad (2.53)$$

$$C_n = 2.28 + 0.924/n. \quad (2.54)$$

The constant C_n takes values 8.74, 9.71, 10.6 and 11.5 for $n=1/7$, $1/8$, $1/9$ and $1/10$, respectively [41, 80, 130, 138, 139]. Approximation (2.54) was obtained in the work [69].

In works [73–75], a modified velocity $V_* = \omega r |\beta - 1| [1 + (\alpha + \kappa)^2]^{1/2}$ was used that, with no real justification of such a choice, only complicated all the mathematical derivations.

One should also mention the model [52], which employed logarithmic approximations for the velocity profiles. In frames of this approach, one has near the wall

$$v_r = \alpha\omega r + \frac{2.5\alpha V_\tau}{(1 + \alpha^2)^{1/2}} \ln(\xi), \quad v_\varphi = -\frac{2.5V_\tau}{(1 + \alpha^2)^{1/2}} \ln(\xi). \quad (2.55)$$

Approach (2.55) was validated only for the free disk case; the heat transfer problem has not been solved. An algebraic equation for the moment coefficient C_M obtained in the work [52] (see Sect. 3.3) is transcendental. Namely because of its excessive complexity and inconvenience, the logarithmic approach [52] has not been widely used further.

2.3.2 Thermal Boundary Layer

In the majority of the known works [41, 68, 72–77, 80, 114, 130, 133, 135, 138, 139, 196], heat transfer modelling in frames of the integral method has been performed with the help of a theory of local modelling. For the first time, this theory was applied to rotating-disk systems by Dorfman [41], who used for this purpose the method of Loytsyanskiy [113]. According to the theory of local modelling, a heat

transfer law determining variation of the Stanton number has the following form [41, 82]:

$$St = M_s Re_T^{**-\sigma} Pr^{-n_s}, \quad (2.56)$$

where M_s , σ and n_s are universal constants independent of the Prandtl number and temperature distribution T_w on the disk surface. For turbulent flow, the constants in Eq. (2.56) have the values $\sigma=0.25$, $n_s=0.5$ and $M_s=7.246 \cdot 10^{-3}$; for laminar flow, these constants are equal to $\sigma=1.0$, $n_s=1.0$ and $M_s=0.07303$ [41, 89, 138, 139]. Relation (2.56) allows closing the thermal boundary layer equation (2.28), where the value δ_T^{**} becomes the only unknown.

Instead of the enthalpy thickness δ_T^{**} , the authors of the work [138, 139] employed the Reynolds analogy parameter χ defined as

$$\frac{q_w}{\tau_{w\varphi}} = \chi \frac{c_p(T_\infty - T_w)}{\omega r(1 - \beta)}. \quad (2.57)$$

Using model (2.56) and definition (2.57), the authors of [138, 139] solved Eq. (2.28) to find the unknown value of χ .

For a long time, the work [122] had been the only one that involved a power-law approximation of the temperature profile in turbulent flow

$$\Theta = \frac{T - T_w}{T_\infty - T_w} = \xi_T^{n_T}, \quad \theta = \frac{T - T_\infty}{T_w - T_\infty} = 1 - \Theta = 1 - \xi_T^{n_T} \quad (2.58)$$

at $n_T=1/5$. Authors of [122] used an unjustified additional correlation $\Delta = \delta_T/\delta = 6$ at $T_w=const$ and did not offer a model to derive dependence of the parameter Δ on the factors affecting heat transfer, which could become an alternative to the approach based on Eq. (2.56).

2.4 Integral Method for Modelling Fluid Flow and Heat Transfer in Rotating-Disk Systems

2.4.1 Structure of the Method

A series of original results of investigations into fluid flow and heat transfer in rotating-disk systems presented in this monograph were obtained with the help of an improved integral method developed by the author of the monograph [163–181, 184, 189, 190]. This method will be referred to as *the present integral method* throughout the monograph.

The present integral method is based on using the following:

- (a) integral equations (2.22), (2.23), (2.24), (2.25), (2.26), (2.27) and (2.28);
- (b) improved models of the turbulent velocity and temperature profiles;
- (c) a novel model for the enthalpy thickness in laminar flow;

- (d) closing relations for the shear stresses and heat fluxes on the disk surface;
- (e) boundary conditions for the velocity and temperature outside of the boundary layer, as well as for the disk surface temperature.

The key point of the present integral method consists in using the same approach to model both laminar and turbulent flow regimes. The only difference consists in the particular values of the certain numerical coefficients involved in the model. Such an approach is in fact a development of the idea of Loytsyanskiy [113], who noticed an analogy between the main parameters of the laminar and turbulent boundary layers subjected to the same boundary conditions. This idea has already proved its fruitfulness in the problems of convective heat transfer in rotating-disk systems. It has already been used by the authors of the works [41, 80, 138, 139]; however, the approach employed in these works in view of its intrinsic imperfectness lead to significant inaccuracy in modelling of some heat transfer regimes (see Sect. 3.2).

An important feature of the present integral method is understanding the fact that any power-law approximation of the velocity and temperature profiles in laminar flow requires using polynomials of not less than the seventh order. In its turn, this leads to deriving cumbersome and inconvenient relations for the Nusselt number and the friction coefficient. On the other hand, simple power-law approximations of the velocity and temperature profiles for turbulent flow result in quite simple and lucid relations for the rest of the boundary layer characteristics including the Nusselt number and the enthalpy thickness. Having obtained, on this basis, the mathematical form of the necessary parameters for turbulent flow, it is rather easy to extend these formulas onto laminar flow under an assumption that certain coefficients are deemed to be unknowns to be found empirically from comparisons with the self-similar exact solution. As shown below, this method proved to be the most accurate among all the known integral methods for the rotating-disk systems.

Therefore, the logical sequence of developing the integral method below is as follows. First, the integral method for turbulent flow will be developed and thoroughly validated. Second, the integral method will be extended and validated for laminar flow conditions.

2.4.2 Turbulent Flow: Improved Approximations of the Velocity and Temperature Profiles

For modelling of the velocity profiles, we will use power-law approximations, namely, Eq. (2.42) for v_r , Eqs. (2.43) (the first one) and (2.45) for v_φ . The function $\tan\varphi$ is specified in the form of a quadratic parabola, whose coefficients a , b and c can be found using the boundary conditions on a disk and on the outer boundary of the boundary layer:

$$\tan\varphi = a + b\xi + c\xi^2, \quad (2.59)$$

$$\xi = 0, \quad \tan\varphi = \tan\varphi_w = \alpha, \quad (2.60)$$

$$\xi = 1, \quad \tan\varphi = \tan\varphi_\infty = v_{r,\infty}/(\omega r - v_{\varphi,\infty}) = N/(1 - \beta) = \kappa, \quad (2.61)$$

$$\xi = 1, \quad d(\tan\varphi)/d\xi = 0. \quad (2.62)$$

Based on this, one can obtain that

$$a = \alpha, \quad b = -2(\alpha - \kappa), \quad c = \alpha - \kappa, \quad (\tan\varphi - \kappa)/(\alpha - \kappa) = (1 - \xi)^2. \quad (2.63)$$

Profiles of the velocity components \bar{v}_r and \bar{v}_φ for a free rotating disk ($\kappa=0$) computed by Eqs. (2.42) and (2.63) are depicted in Figs. 2.2 and 2.3.

Wall values of the tangent of the flow swirl angle α depending on the exponent n were determined with the help of the present integral method and documented below in Table 3.4 devoted to a free rotating disk. Also presented in Table 3.4 are numerical data for α obtained using von Karman's method [80]. Advantages of the power-law model for the \bar{v}_r and \bar{v}_φ profiles jointly with the quadratic approximation of $\tan\varphi$ in the form of Eq. (2.63) are obvious: it provides computational results that agree well with the experimental data in the outer region of the boundary layer, with the profiles at $n=1/9$ being in best agreement with the experimental data [63, 111] (Figs. 2.2 and 2.3). The same conclusion follows from Fig. 2.4, where the radial and tangential velocities are interrelated using an equation obtained from Eqs. (2.42), (2.43), (2.45) and (2.63) [163]

$$\bar{v}_r = \alpha \bar{v}_\varphi (1 - \bar{v}_\varphi^{1/n})^L, \quad (2.64)$$

where $L=2$ for the present integral method and $L=1$ for the von Karman's method [80] (although, in the near-wall region, the closest agreement between the profiles is observed for $n=1/7-1/8$). From Eq. (2.64), a maximum in the dependence of \bar{v}_r on \bar{v}_φ can also be obtained in the following form [163]:

$$\bar{v}_{\varphi, \max} = \xi_{\max}^n, \quad \xi_{\max} = n/(n + L). \quad (2.65)$$

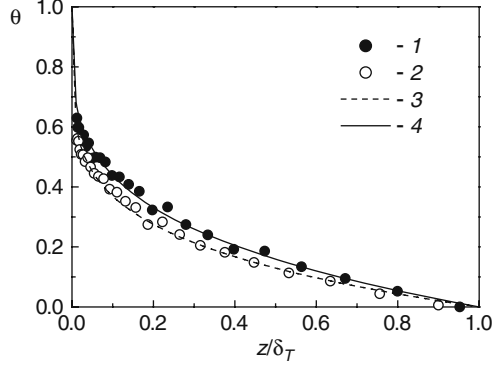
Equation (2.63) is a generalization of the quadratic relation (2.47) proposed for the case $\kappa=0$. Somewhat worse agreement of Eq. (2.47) with experimental data mentioned in the works [118, 196] may have been caused by a less accurate choice of the constants n and α .

Temperature profiles in the boundary layer have been approximated with the power law, Eq. (2.58), which agrees well with known experiments (see Fig. 2.5).

2.4.3 Models of Surface Friction and Heat Transfer

Relations for the shear stresses $\tau_{w\varphi}$, τ_{wr} and wall heat flux q_w will be found with the help of a two-layer model of the velocity and temperature profiles in the wall

Fig. 2.5 Profiles of the non-dimensional temperature θ in the turbulent boundary layer over a free rotating disk. Experiments [46], $q_w = \text{const}$, $Re_\omega = 1.0 \cdot 10^6$: 1 – inner heater on, 2 – inner heater off. Calculations by Eq. (2.58): 3 – $n_T = 1/5$, 4 – $1/4$.



coordinates. It is obvious that in the region where the power-law profiles (2.45) and (2.58) are in force, one can rewrite these profiles as follows:

$$V^+ = \xi^n / \sqrt{c_f/2}, \quad T^+ = \xi_T^{n_T} \sqrt{c_f/2} / St. \quad (2.66)$$

Since these power-law equations do not hold in the viscous sub-layer, they are replaced here with the following equations:

$$V^+ = z^+, \quad T^+ = Pr z^+. \quad (2.67)$$

Splicing relations (2.66) and (2.67) at the boundary of the viscous sub-layer (at the coordinate z_1^+) and heat conduction sub-layer (at the coordinate z_{1T}^+) and transforming, one can finally obtain formulas for the surface friction coefficient and the Stanton number

$$c_f/2 = (z_1^+)^{2(n-1)/(n+1)} \cdot Re_{V_*}^{-2n/(n+1)}, \quad (2.68)$$

$$St = (z_1^+)^{n_T-1} Re_{V_*}^{-n_T} (c_f/2)^{(1-n_T)/2} \Delta^{-n_T} (z_{1T}^+/z_1^+)^{n_T-1} Pr^{-n_T}. \quad (2.69)$$

The value of z_1^+ most often used in a modified form of the coefficient $C_n = (z_1^+)^{1-n}$ is a constant depending only on the exponent n (see Eq. (2.54)) [41, 130, 138, 139]. The interrelation among shear stresses τ_w , $\tau_{w\varphi}$ and τ_{wr} is defined by Eqs. (2.52). Taking this into account

$$\begin{aligned} \tau_{wr}/\rho &= C_n^{-2/(n+1)} \text{sgn}(1-\beta)(v/\delta)^{2n/(n-1)}(\omega r|1-\beta|)^{2/(n-1)}\alpha(1+\alpha^2)^{0.5(1-n)/(1+n)}, \\ \tau_{w\varphi}/\rho &= -C_n^{-2/(n+1)} \text{sgn}(1-\beta)(v/\delta)^{2n/(n-1)}(\omega r|1-\beta|)^{2/(n-1)}(1+\alpha^2)^{0.5(1-n)/(1+n)}. \end{aligned} \quad (2.70)$$

The ratio (z_{1T}^+/z_1^+) is a function of the Prandtl number only; the quantity Δ (the unknown to be found) depends on the boundary condition for $T_w(r)$ and the Prandtl number Pr . Let us denote $(z_{1T}^+/z_1^+)^{n_T-1} Pr^{-n_T} = Pr^{-n_p}$, where the constant n_p remains unknown as yet.

In the majority of the solutions below, an assumption $\pi_T = n$ will be used. In this case, formulas for the Stanton and the Nusselt number take the following form:

$$St = (c_f/2)\Delta^{-n}Pr^{-n_p}, \quad (2.71)$$

$$Nu = St \frac{V_* r}{\nu} Pr = St Re_\omega Pr |\beta - 1| (1 + \alpha^2)^{1/2}. \quad (2.72)$$

2.4.4 Integral Equations with Account for the Models for the Velocity and Temperature Profiles

Integration of Eqs. (2.22) and (2.23) with respect to the coordinate z with allowance for relations (2.42), (2.43), (2.44) and (2.45) and (2.63) yields the following result [163]:

$$\begin{aligned} & \frac{d}{dr} \left\{ \delta r (\omega r)^2 (1 - \beta)^2 \left[\kappa (A_1 \alpha + A_2 \kappa) - (B_1 \alpha^2 + B_2 \alpha \kappa + B_3 \kappa^2) \right] \right\} + \\ & \delta \omega r^2 (1 - \beta) \frac{d(N\omega r)}{dr} [\kappa - (A_1 \alpha + A_2 \kappa)] + \rho \delta (\omega r)^2 (C_1 + C_2 \beta + C_3 \beta^2) \\ & = r \tau_{wr} / \rho, \end{aligned} \quad (2.73)$$

$$\begin{aligned} & \frac{d}{dr} \left\{ \delta \omega^2 r^4 (1 - \beta) [\alpha (D_1 + \beta D_2) + \kappa (D_3 + \beta D_4)] \right\} \\ & - (\omega r)^2 \beta \frac{d}{dr} [\delta \omega r^2 (1 - \beta) (A_1 \alpha + A_2 \kappa)] = -r^2 \tau_{w\varphi} / \rho, \end{aligned} \quad (2.74)$$

where $A_1 = 1/(n+1) - A_2$; $A_2 = 2/(n+2) - 1/(n+3)$;
 $B_1 = 1/(2n+1) - 2/(n+1) + 6/(2n+3) - 2/(n+2) + 1/(2n+5)$;
 $B_2 = 2/(n+1) - 10/(2n+3) + 4/(n+2) - 2/(2n+5)$; $D_1 = A_1 - D_2$;
 $C_1 = -2/(n+1) - C_3$, $C_2 = -2(1/(2n+1) - 1/(n+1))$; $C_3 = -1 + 1/(2n+1)$;
 $D_1 = A_1 - D_2$; $D_2 = 1/(2n+1) - D_4$; $D_3 = A_2 - D_4$; $D_4 = 1/(n+1) - 1/(2n+3)$.

The thermal boundary layer equation (2.25), being integrated with respect to the coordinate z with allowance for Eqs. (2.42), (2.43), (2.45), (2.58) and (2.63), can be reduced to the following form [168]:

$$\begin{aligned} & \frac{d}{dr} [\delta \omega r^2 (1 - \beta) F_1 (T_\infty - T_w)] + \frac{dT_\infty}{dr} \delta \omega r^2 (1 - \beta) F_2 =, \\ & = -St V_* r \Delta^{-n_T} Pr^{-n_p} (T_\infty - T_w) \end{aligned} \quad (2.75)$$

where $F_1 = E_1$, $F_2 = E_2$ at $\Delta \leq 1$; $F_1 = E_3$, $F_2 = E_4$ at $\Delta \geq 1$;

$$E_1 = \Delta^{n+1} (aa_{*T} + bb_{*T} \Delta + cc_{*T} \Delta^2),$$

$$a_{*T} = 1/(1+n+n_T) - 1/(1+n),$$

$$b_{*T} = 1/(2+n+n_T) - 1/(2+n),$$

$$c_{*T} = 1/(3+n+n_T) - 1/(3+n),$$

$$E_2 = \Delta^{n+1} [a/(n+1) + b\Delta/(n+2) + c\Delta^2/(n+3)],$$

$$E_3 = E_5 + \kappa E_6,$$

$$\begin{aligned}
E_4 &= \alpha A_1 + \kappa(\Delta - 1) + \kappa A_2, \\
E_5 &= \alpha(-A_1 + \Delta^{-n_T} D_{2T}), \\
D_{2T} &= 1/(1 + n + n_T) - D_{4T}, \\
E_6 &= (\Delta - \Delta^{-n_T})/(n_T + 1) - \Delta + 1 - A_2 + \Delta^{-n_T} D_{4T}, \\
D_{4T} &= 2/(2 + n + n_T) - 1/(3 + n + n_T).
\end{aligned}$$

Mass flowrate in the boundary layer can be calculated from the following relation:

$$\dot{m}_d / (\rho \omega r^3) = 2\pi(1 - \beta)(A_1 \alpha + A_2 \kappa) \delta / r. \quad (2.76)$$

As applied to the problems under consideration, Eqs. (2.73), (2.74) and (2.75) contain three unknowns:

- (a) *in the entraining boundary layers*: α , δ and Δ for given β and T_∞ ;
- (b) *in the Ekman-type boundary layers*: α , β for a given distribution of δ (i.e. for a constant mass flowrate \dot{m}_d) and T_∞ for a given constant value Δ .

In the former case for particular boundary conditions (2.32), (2.33), (2.34), (2.35) and (2.36) (and $N = \text{const}$), Eqs. (2.73), (2.74) and (2.75) can be solved analytically at constant values α and Δ and power law of radial variation of the boundary layer thickness δ . For arbitrary boundary conditions, Eqs. (2.73), (2.74) and (2.75) are solved numerically; for the sake of this, they are reduced to a form convenient for integration using the Runge-Kutte method [164, 169]:

$$\begin{cases} \alpha' = (\Phi_1 \Phi_4 + \Phi_2)/(1 - \Phi_1 \Phi_3), \\ \bar{\delta}' = (\Phi_2 \Phi_3 + \Phi_4)/(1 - \Phi_1 \Phi_3), \end{cases} \quad (2.77)$$

$$\Delta' = (S_1 - S_2 - S_3)/S_4. \quad (2.78)$$

Here

$$\begin{aligned}
\Phi_2 &= \{[\text{sgn}(1 - \beta) |c_{fr}/2| \bar{r}^3 Re_{V_*}^2 / \bar{\delta}^2 - Z_1 \bar{\delta} - G_1 \bar{\delta} - G_2]/(\bar{\delta} \bar{r}) - Q_2 \bar{r}^2\} / Q_1; \\
\Phi_4 &= \{-\text{sgn}(1 - \beta) |c_{f\varphi}/2| \bar{r}^2 Re_{V_*}^2 / \bar{\delta}^2 - \bar{\delta}[\alpha Q'_3 + \bar{Q}'_4 + (\beta Re_\omega)'(\alpha Q_5 + Q_6)]/Q_7\}; \\
\Phi_1 &= -Z_1/(\bar{\delta} Q_1); \Phi_3 = -\bar{\delta} Q_3/Q_7; G_1 = Re_\omega^2(C_1 + C_2 \beta + C_3 \beta^2); \\
Z_1 &= Re_\omega^2(1 - \beta)^2[-B_1 \alpha^2 + \alpha \kappa(A_1 - B_2) + \kappa^2(A_2 - B_3)]; G_2 \\
&= Re_\omega^2(1 - \beta) \bar{\delta}[-A_1 \alpha + \kappa(1 - A_2)] \bar{v}'_{r,\infty}; \\
Q_1 &= Re_\omega^2(1 - \beta)^2[-2\alpha B_1 + \kappa(A_1 - B_2)]; \\
Q_2 &= Re_{\omega i}^2\{-\alpha^2 B_1[\bar{r}^2(1 - \beta)^2]' + \alpha(A_1 - B_2)[\bar{r}(1 - \beta) \bar{v}_{r,\infty}]' + (A_2 - B_3)(\bar{v}_{r,\infty}^2)'\}; \\
Q_3 &= -Re_\omega^2(1 - \beta)^2 D_1; Q_4 = -Re_\omega^2(1 - \beta) \bar{v}_{r,\infty} D_3/\bar{r}; Q_5 = -Re_\omega(1 - \beta) A_1; \\
Q_6 &= -Re_{\omega i} \bar{r} \bar{v}_{r,\infty} A_2; \\
Q_7 &= \alpha Q_3 + Q_4; \bar{v}_{r,\infty} = \bar{v}_{r,\infty}/(\omega a); Re_{\omega i} = \omega r_i^2/\nu; |c_{fr}/2| \\
&= (c_f/2)\alpha/(1 + \alpha^2)^{1/2}; \\
|c_{f\varphi}/2| &= (c_f/2)/\alpha/(1 + \alpha^2)^{1/2} \quad \bar{\delta} = \delta/r_i; \bar{r} = r/r_i.
\end{aligned}$$

In Eq. (2.78), one has at $\Delta \leq 1$:

$$\begin{aligned} S_1 &= -Re_\omega |1 - \beta| (1 + \alpha^2)^{1/2} St (\bar{T}_\infty - \bar{T}_w); \\ S_2 &= \bar{T}'_\infty \bar{\delta} Re_\omega \Delta^{n+1} [\alpha(1 - \beta)/(n + 1) - 2\Delta(\alpha(1 - \beta) - N)/(n + 2) \\ &\quad + \Delta^2(\alpha(1 - \beta) - N)/(n + 3)]; \\ S_3 &= \Delta^{n+1} L'_1 + \Delta^{n+2} L'_2 + \Delta^{n+3} L'_3; \\ S_4 &= L_1(n + 1)\Delta^n + L_2(n + 2)\Delta^{n+1} + L_3(n + 3)\Delta^{n+2}; \\ L_1 &= L_0 a_{*T} \alpha(1 - \beta); \\ L_2 &= L_0 b_{*T} (-2)[\alpha(1 - \beta) - N]; \\ L_3 &= L_0 c_{*T} [\alpha(1 - \beta) - N]; \\ L_0 &= \bar{\delta} Re_\omega (\bar{T}_\infty - \bar{T}_w). \end{aligned}$$

The value of S_1 is the same for both $\Delta \geq 1$ and $\Delta \leq 1$.

At $\Delta \geq 1$:

$$\begin{aligned} S_2 &= \bar{T}'_\infty \bar{\delta} Re_\omega [\alpha(1 - \beta)A_1 + NA_2 + N(\Delta - 1)]; \\ S_3 &= L'_1 C_{6T}^* + L'_2 C_{7T}^*; \\ S_4 &= -n_T \Delta^{-n_T-1} D_{2T} L_{1*} + [(1 + n_T \Delta^{-n_T-1})/(n_T + 1) - D_{4T} n_T \Delta^{-n_T-1} - 1] L_{2*}; \\ L_{1*} &= L_0 (1 - \beta) \alpha; \\ L_{2*} &= L_0 N; \\ C_{6T}^* &= -A_1 + \Delta^{-n_T} D_{2T}; \\ C_{7T}^* &= (\Delta - \Delta^{-n_T})/(n_T + 1) - \Delta + 1 - A_2 + D_{4T} \Delta^{-n_T}; \\ \bar{T} &= T/T_{ref}. \end{aligned}$$

The primes denote here derivatives with respect to the radial coordinate $d/d\bar{r}$; r_i is a characteristic radius (very often, the inlet radius).

In the Ekman-type layers

$$\begin{cases} \alpha' = \frac{c_f}{2} \alpha (\beta - 1) Re_\omega (1 + \alpha^2)^{1/2} \frac{4\pi A_1 r_i}{B_1 C_w b} + \frac{d\beta}{d\bar{r}} \frac{\alpha}{\beta - 1} - \frac{C_3 [\beta + n/(n+1)]}{\bar{r}(\beta - 1)\alpha B_1} - \frac{\alpha}{\bar{r}}, \\ \beta' = \left\{ -\frac{c_f}{2} (1 - \beta)^2 Re_\omega (1 + \alpha^2)^{1/2} \frac{4\pi A_1 r_i}{D_1 C_w b} - \frac{2}{\bar{r}} \left[\beta \left(1 - \frac{A_1}{D_1} \right) - 1 \right] \right\} / \left(1 - \frac{A_1}{D_1} \right), \end{cases} \quad (2.79)$$

$$\frac{d\bar{T}_\infty}{d\bar{r}} = \left[St \frac{V_* r}{\nu} \frac{2\pi}{0.5 C_w} \frac{r_i}{b} \frac{1}{K_H} (\bar{T}_\infty - \bar{T}_w) + \frac{d\bar{T}_w}{d\bar{r}} \right] \frac{K_H}{K_H - 1}. \quad (2.80)$$

According to the recommendations of [138, 139], parameter K_H is considered to be constant in the Ekman-type layers [164, 167, 170]

$$K_H = 1 - (D_{2T}/A_1) \Delta^{-n_T} = \text{const} \quad \text{or} \quad \Delta = \text{const}. \quad (2.81)$$

2.5 General Solution for the Cases of Disk Rotation in a Fluid Rotating as a Solid Body and Simultaneous Accelerating Imposed Radial Flow

Let us consider the case where $\beta = \text{const}$, $N = \text{const}$ and $\kappa > 0$. The condition $\beta = \text{const}$ means solid-body rotation, which takes place between rotors and stators; the condition $N = \text{const}$ means accelerating radial flow that exists in the stagnation region

of fluid flow impinging on an orthogonal surface; the condition $\kappa > 0$ means that recirculation flow does not emerge on a rotating disk [138, 139, 196]. Under these conditions, the system of Eqs. (2.73) and (2.74) can be solved analytically in the most general form [174, 180, 189]:

$$\delta = C_\delta r^m, \quad C_\delta = \gamma(\omega/\nu)^{-2n/(3n+1)}, \quad \delta/r = \gamma Re_\omega^{-2n/(3n+1)}, \quad (2.82)$$

$$\alpha = \text{const}, \quad m = (1 - n)/(3n + 1), \quad (2.83)$$

$$\gamma = \gamma_* |1 - \beta|^{(1-n)/(3n+1)}, \quad (2.84)$$

$$C_M = \varepsilon_M Re_\phi^{-2n/(3n+1)}, \quad (2.85)$$

$$\dot{m}_d/(\mu r) = \varepsilon_m Re_\omega^{(n+1)/(3n+1)}, \quad (2.86)$$

$$c_f/2 = A_c Re_\omega^{-2n/(3n+1)}, \quad (2.87)$$

$$\alpha = -H_2/2H_3 + [(H_2/2H_3)^2 - H_1/H_3]^{1/2}, \quad (2.88)$$

$$\gamma_* = C_n^{-2/(3n+1)} (1 + \alpha^2)^{0.5(1-n)/(3n+1)} H_9^{-(n+1)/(3n+1)}, \quad (2.89)$$

$$\varepsilon_m = \varepsilon_m^* |1 - \beta|^{2(n+1)/(3n+1)}, \quad \varepsilon_m^* = 2\pi \gamma (A_1 \alpha + A_2 \kappa) \text{sgn}(1 - \beta), \quad (2.90)$$

$$\varepsilon_M = \frac{8\pi}{5 - 4n/(3n + 1)} C_n^{-\frac{2}{n+1}} \gamma_*^{\frac{2n}{n+1}} |1 - \beta|^{\frac{2(n-1)}{3n+1}} (1 + \alpha^2)^{\frac{1-n}{2(n+1)}} \text{sgn}(1 - \beta), \quad (2.91)$$

$$A_c = C_n^{-2/(n+1)} \gamma^{-2n/(n+1)} (1 + \alpha^2)^{-n/(n+1)} |\beta - 1|^{-2n/(n+1)}, \quad (2.92)$$

where $H_1 = C_3(\beta - C_5) + (\beta - 1)\kappa^2 H_4$; $H_2 = \kappa(\beta H_5 + H_6)$; $H_3 = \beta H_7 + H_8$; $H_4 = 1 + (2+m)A_2 - (3+m)B_3$; $H_5 = A_1(2+m) - B_2(3+m) + D_4(m+4) - A_2(2+m)$; $H_6 = -A_1(2+m) + B_2(3+m) + D_3(4+m)$; $H_7 = -(3+m)B_1 + (4+m)D_2 - (2+m)A_1$; $H_8 = (3+m)B_1 + (4+m)D_1$; $C_5 = C_1/C_3$; $H_9 = \alpha[(D_1 + \beta D_2)(4+m) - \beta(2+m)A_1] + \kappa[(D_3 + \beta D_4)(4+m) - \beta A_2(2+m)]$.

An analytical solution of Eq. (2.75) is possible only under assumptions of $\Delta = \text{const}$, $Pr = \text{const}$, $n = n_T$ and boundary conditions (2.34), (2.35) and (2.36). It is evident that in this case $D_{2T} = D_2$ and $D_{4T} = D_4$.

Substituting Eqs. (2.36), (2.72), (2.82) and (2.83) into Eq. (2.75) and solving it jointly with Eq. (2.74), one can obtain [168] that

$$\left[F_1 (2 + m + n_*) + \frac{\beta n_*}{\beta - 1} F_2 \right] \Delta^n Pr^{n_p} = (4 + m)C_4 + \frac{2\beta}{\beta - 1} C_5. \quad (2.93)$$

The relations for the functions F_1 and F_2 are given in explanations to Eq. (2.75), while $C_4 = -(\alpha D_1 + \kappa D_2)$, $C_5 = 1/(n+1) + 1/(n+2) + 1/(n+3)$. Equation (2.93) has different solutions for the cases $\Delta \geq 1$ and $\Delta \leq 1$ (which is reflected by the different forms of the functions F_1 and F_2 for $\Delta \geq 1$ and $\Delta \leq 1$). Case $\Delta \geq 1$ corresponds to

heat transfer in gases at $Pr \leq 1$. Case $\Delta \leq 1$ corresponds, in general, to heat transfer in liquids at $Pr \geq 1$; more details relevant to the case where $\Delta \leq 1$ can be found in Chap. 8.

Solution (2.93) in its general form for simultaneously non-zero values of β and N is a transcendental algebraic equation. A solution for the parameter Δ in an explicit form can be obtained at $N=0$ and $\Delta \geq 1$. The exponent n_p , which is considered universally the same for all types of fluid flow, will be found below on analysis of the free rotating disk case.

Expressions for the Nusselt and Stanton numbers have the following form:

$$St = A_c Re_\omega^{-2n/(3n+1)} \Delta^{-n} Pr^{-n_p}, \quad (2.94)$$

$$Nu = A_c (1 + \alpha^2)^{1/2} |1 - \beta| Re_\omega^{(n+1)/(3n+1)} \Delta^{-n} Pr^{1-n_p}. \quad (2.95)$$

Validations of the *present integral method* are performed in Chaps. 3, 5 and 6 for air flows. Extension of the present integral method onto the laminar flow case is performed in Chaps. 3 and 5. Chapter 3 represents results for a free rotating disk ($\beta=0$, $N=0$). Analysed in Chap. 5 are the cases of a disk rotating in a fluid that itself rotates as a solid body ($\beta=const$, $N=0$) and a disk rotating in a uniformly accelerating non-rotating fluid ($\beta=0$, $N=const$). Chapter 6 represents results for turbulent throughflow between parallel co-rotating disks. In Chap. 8, the method is validated for cases of Prandtl or Schmidt numbers larger than unity.

Convective Heat and Mass Transfer in Rotating Disk
Systems

Shevchuk, I.V.

2009, XIX, 236 p. 116 illus., Hardcover

ISBN: 978-3-642-00717-0